Spontaneous time-reversal symmetry breaking by disorder in superconductors

Brian M. Andersen[1]*, Andreas Kreisel[1] and P. J. Hirschfeld[2]

[1]Niels Bohr Institute, University of Copenhagen, Copenhagen, Denmark, [2]Department of Physics, University of Florida, Gainesville, FL, United States

A growing number of superconducting materials display evidence for spontaneous time-reversal symmetry breaking (TRSB) below their critical transition temperatures. Precisely what this implies for the nature of the superconducting ground state of such materials, however, is often not straightforward to infer. We review the experimental status and survey different theoretical mechanisms for the generation of TRSB in superconductors. In cases where a TRSB complex combination of two superconducting order parameter components is realized, defects, dislocations and sample edges may generate superflow patterns that can be picked up by magnetic probes. However, even single-component condensates that do not break time-reversal symmetry in their pure bulk phases can also support signatures of magnetism inside the superconducting state. This includes, for example, the generation of localized orbital current patterns or spin-polarization near atomic-scale impurities, twin boundaries and other defects. Signals of TRSB may also arise from a superconductivity-enhanced Ruderman-Kittel-Kasuya-Yosida exchange coupling between magnetic impurity moments present in the normal state. We discuss the relevance of these different mechanisms for TRSB in light of recent experiments on superconducting materials of current interest.

KEYWORDS

time-reversal symmetry breaking, superconductivity, disorder, condensed matter theory, quantum materials

1 Introduction

Several superconducting materials have been discovered to manifest evidence of spontaneous time-reversal symmetry breaking (TRSB) that appears only below their critical superconducting transition temperatures T_c [1–4]. Evidence for such TRSB originates mainly from an enhanced muon-spin relaxation (μSR) and/or polar Kerr effect measurements finding a change in the optical polar Kerr angle below T_c. Additional probes able to detect breaking of time-reversal symmetry in the superconducting phase include Josephson interferometry [5], superconducting quantum interference device (SQUID) magnetometry [6], and polarized and small-angle neutron scattering [7]. These experimental methods detect the internal magnetic fields spontaneously generated in the superconducting state. Explanations for the occurrence of such fields from the perspective of clean (homogeneous) physical effects are either in terms of a TRSB non-unitary spin-triplet pairing state or in terms of multi-component superconducting condensates entering a complex TRSB superposition of two superconducting order parameter components. The latter option is particularly natural for superconducting instabilities condensing in two-dimensional (2D) irreducible representations of the associated crystal point group. Complex superpositions of two

symmetry-distinct order parameters break TRSB, and generate persistent supercurrent patterns at material edges, dislocations, or around various defect sites, which produce magnetic fields that may not average to zero locally. Such a multi-component scenario for the origin of TRSB below T_c has been extensively discussed for e.g., Sr_2RuO_4 [4, 8–12], UPt_3 [13, 14], URu_2Si_2 [15], UTe_2 [16, 17], $SrPtAs$ [18], Re [19], Zr_3Ir [20], $LaNiC_2$ [21], $LaNiGa_2$ [22], $PrOs_4Sb_{12}$ [23, 24], $Ba_{1-x}K_xFe_2As_2$ [25, 26], $FeSe_{1-x}S_x$ [27], and more recently also for the kagome superconductors AV_3Sb_5 (A: K, Rb, Cs) [28–30], $4Hb$-TaS_2 [31], $CaPd_2Ge_2$ [32], skutterudites [33, 34] and $Na_2Cr_3As_3$ [35]. For most of the compounds listed here, the evidence for TRSB originates from μSR experiments. For further materials displaying TRSB in their superconducting phases, and other types of evidence, we refer to Refs. [1–4].

At present, the status of the precise superconducting ground state remains controversial for many of the materials listed above. This is the case, for example, for the two materials Sr_2RuO_4 and UTe_2, where specific heat data features only a single thermodynamic transition that does not split under uniaxial strain, casting considerable doubt on the multi-component nature of their superconducting condensates [36–39]. Therefore, it appears timely and important to pursue other possibilities for the origin of TRSB detected solely inside the superconducting phase. This motivates the question of what mechanisms there are for TRSB of superconducting condensates composed of a single component order parameter? Barring non-unitary TRSB spin-triplet order, the answer to this question naturally leads to a study of different forms of spatial inhomogeneities and their influence on the local properties of superconductivity. For example, it is known that some superconductors generate magnetic moments below T_c due to an interplay between the gap structure and electronic correlations [40–46]. As mentioned above, another possibility for TRSB appearing only below T_c includes the generation of localized orbital loops of supercurrents near impurities. The latter is well-known to arise near nonmagnetic disorder sites in complex TRSB multi-component condensates [47–54], but was recently shown to be also present in the strongly disordered regime of single-component superconductors [55, 56]. Likewise, one might expect dislocations and grain boundaries to similarly operate as seeds of localized supercurrents producing sizable internal magnetic fields. Recently, the latter scenario was studied in Refs. [57, 58] as a possible explanation for reconciling the existence of TRSB and a single specific heat transition in Sr_2RuO_4. Indeed for this material, edge dislocations are known to be prevalent in many samples [59]. Finally, one might also envision that time-reversal symmetry is already broken above T_c through the existence of small magnetic regions that are either too dilute or rapidly fluctuating to be picked up by most probes. Only through a superconductivity-enhanced coupling, or a sufficient slowing-down of such preexisting magnetism below T_c, can it be detected, e.g., by entering the muon relaxation time window.
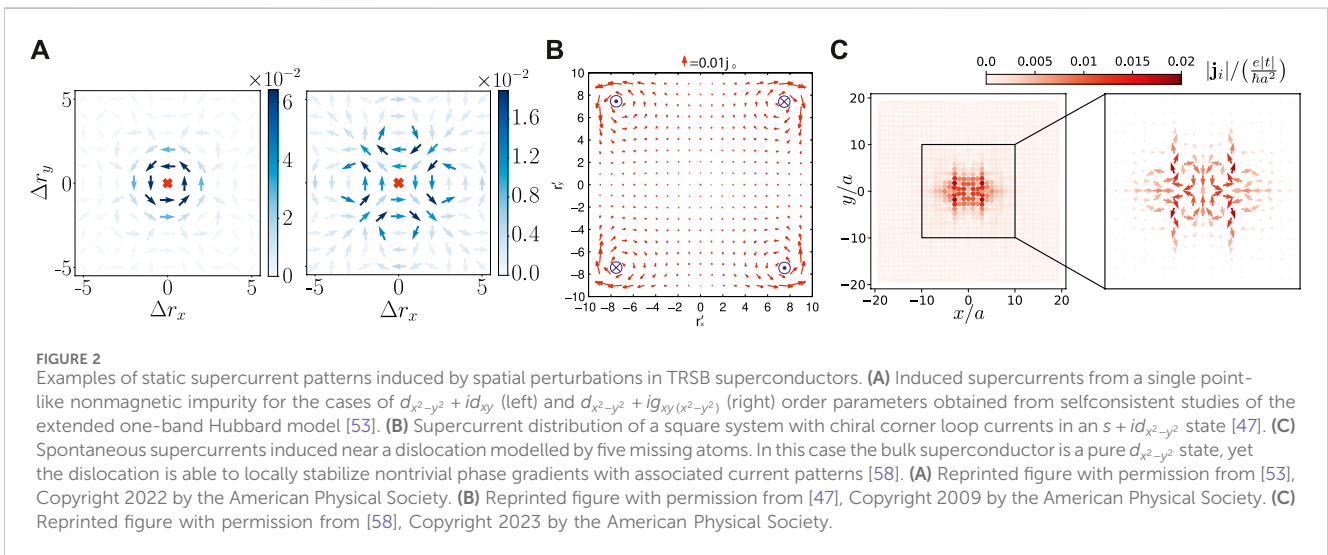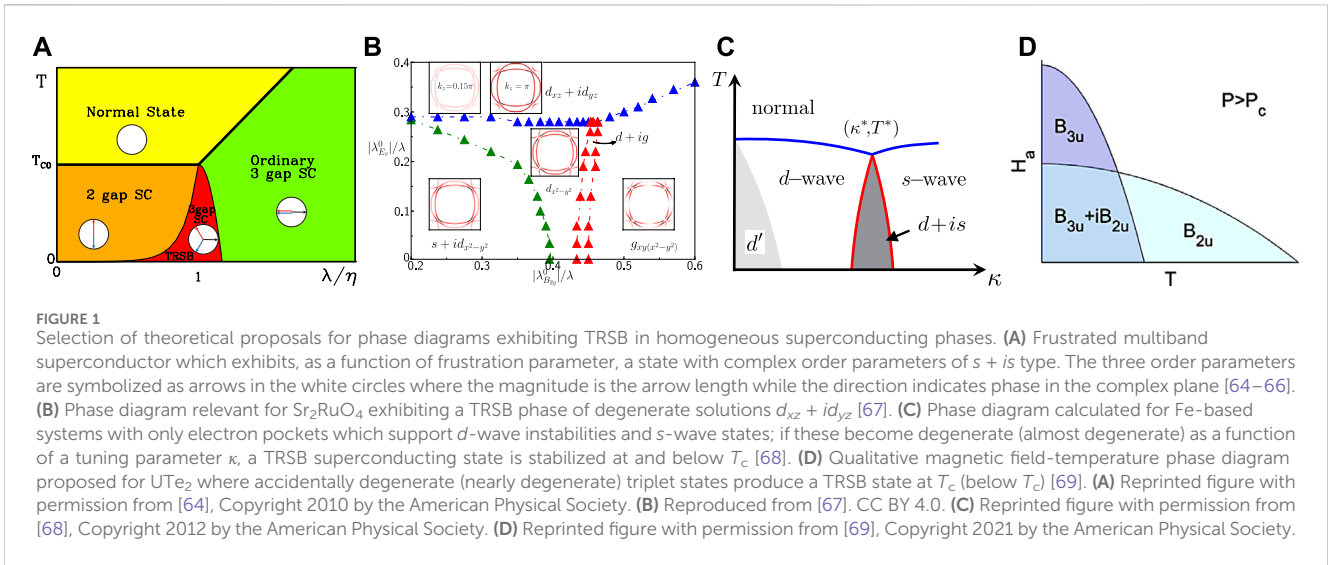
Here, motivated by the above-mentioned developments we survey a number of different mechanisms for *inhomogeneity-induced* TRSB in superconductors. Our discussion of disorder-induced TRSB refers both to cases where TRSB exists only locally near inhomogeneity sites and where TRS is broken globally, but manifested via induced currents near disorder sites. We discuss these both in view of recent theoretical and experimental developments of unconventional superconductivity.

2 Mechanisms of TRSB from disorder in superconductors

In this section we discuss three different mechanisms for disorder-generated TRSB in spin-singlet superconductors. Section 2.1 reviews the generation of magnetic fields from disorder in superconducting phases with TRSB in the bulk or generated near spatial inhomogeneities. Section 2.2 discusses another case where disorder in conjunction with electronic interactions and appropriate superconducting gap structures lead to the generation of static magnetic moments. Due to the required gapping of states for these moments to form, this mechanism is tied to the superconducting phase. Finally, Sec. 2.3 surveys a third case where preexisting magnetic local order (fluctuation moments) in the normal state get enhanced (slowed-down) by superconductivity. Clearly these mechanisms do not exhaust the options for disorder-induced TRSB in superconductors where e.g., cases with substantial spin-orbit coupling may also be of interest [60, 61]. We focus on these three options given recent research along similar lines and for their relevance for some of the superconducting materials mentioned above. For a discussion of the possibility of TRSB in homogeneous superconductors originating from conventional electron-phonon coupling, we refer to the review [3] and the references therein. A theoretical proposal for a mechanism has been proposed in Ref. [62] and recent experimental evidence for TRSB in materials where superconductivity is believed to originate from electron-phonon coupling is reported in Refs. [32–34, 63].

2.1 Complex combinations of two superconducting condensates

Entering the superconducting state is associated with a breaking of the symmetry of the normal state symmetry group composed of a direct product of crystalline symmetries, gauge symmetry and the time reversal operation [70–72]. For non-magnetic normal states, the allowed solutions of the gap equation can be characterized by the irreducible representations (irreps) of the associated point group. The leading instability is found from the linearized BCS gap equation as the solution with the largest eigenvalue and thereby also the highest T_c [73–76]. Broken time-reversal symmetry can arise from a complex combination of superconducting condensates or the breaking of the spin-rotational invariance in non-unitary triplet states. Whenever the preferred superconducting instability corresponds to a two-dimensional (2D) irrep, the system may take advantage of the degeneracy between the representations. From a perspective of the minimization of the Ginzburg–Landau free energy, there is the possibility to either form a real combination thereby breaking a crystal symmetry or to form complex superpositions [3, 12, 71]. The latter often maximizes the condensation energy by forming a fully-gapped state and can be shown to be the ground state for a single band setting within a loop expansion [77]. We will not elaborate further on the possibility of real superpositions, but focus instead on complex linear combinations with standard examples as $p_x + ip_y$ ($p + ip$) chiral order (E_u) in tetragonal systems and $d_{xy} + id_{x^2-y^2}$ ($d + id$) ordered superconductivity (E_2) in hexagonal lattices. Note that by "chiral", we refer to a particular subclass of TRSB superconducting

FIGURE 1
Selection of theoretical proposals for phase diagrams exhibiting TRSB in homogeneous superconducting phases. **(A)** Frustrated multiband superconductor which exhibits, as a function of frustration parameter, a state with complex order parameters of $s + is$ type. The three order parameters are symbolized as arrows in the white circles where the magnitude is the arrow length while the direction indicates phase in the complex plane [64–66]. **(B)** Phase diagram relevant for Sr_2RuO_4 exhibiting a TRSB phase of degenerate solutions $d_{xz} + id_{yz}$ [67]. **(C)** Phase diagram calculated for Fe-based systems with only electron pockets which support d-wave instabilities and s-wave states; if these become degenerate (almost degenerate) as a function of a tuning parameter κ, a TRSB superconducting state is stabilized at and below T_c [68]. **(D)** Qualitative magnetic field-temperature phase diagram proposed for UTe_2 where accidentally degenerate (nearly degenerate) triplet states produce a TRSB state at T_c (below T_c) [69]. **(A)** Reprinted figure with permission from [64], Copyright 2010 by the American Physical Society. **(B)** Reproduced from [67]. CC BY 4.0. **(C)** Reprinted figure with permission from [68], Copyright 2012 by the American Physical Society. **(D)** Reprinted figure with permission from [69], Copyright 2021 by the American Physical Society.

FIGURE 2
Examples of static supercurrent patterns induced by spatial perturbations in TRSB superconductors. **(A)** Induced supercurrents from a single point-like nonmagnetic impurity for the cases of $d_{x^2-y^2} + id_{xy}$ (left) and $d_{x^2-y^2} + ig_{xy(x^2-y^2)}$ (right) order parameters obtained from selfconsistent studies of the extended one-band Hubbard model [53]. **(B)** Supercurrent distribution of a square system with chiral corner loop currents in an $s + id_{x^2-y^2}$ state [47]. **(C)** Spontaneous supercurrents induced near a dislocation modelled by five missing atoms. In this case the bulk superconductor is a pure $d_{x^2-y^2}$ state, yet the dislocation is able to locally stabilize nontrivial phase gradients with associated current patterns [58]. **(A)** Reprinted figure with permission from [53], Copyright 2022 by the American Physical Society. **(B)** Reprinted figure with permission from [47], Copyright 2009 by the American Physical Society. **(C)** Reprinted figure with permission from [58], Copyright 2023 by the American Physical Society.

condensates exhibiting phase winding that breaks mirror symmetries. Along the same lines, solutions of one-dimensional (1D) irreps that are accidentally degenerate may also form such complex superpositions. Such cases are fine tuned, but Fermi surfaces with competing nesting tendencies, for example, are prone to near-degeneracy between several symmetry-distinct superconducting instabilities and may therefore more naturally feature such accidental degenerate superpositions. Examples of these include $d + is$ and $d + ig$ as discussed in the context of iron-based superconductors and Sr_2RuO_4 (see Figures 1B,C), or the so-called $s + is$ state with nontrivial phases on different bands as displayed in the phase diagram in Figure 1A, which also arises as a result of frustrated pairing interactions which are discussed in view of Fe-based superconductors [64–66] and other multiband materials [78]. More recently, accidental degeneracies are also explored for UTe_2 where candidate states include complex spin-triplet superpositions of the form e.g., $A_u + iB_{3u}$, $B_{1u} + iB_{3u}$ or $B_{3u} + iB_{2u}$ now expressed directly in terms of the 1D irreps, see Figure 1D. All the complex superpositions

mentioned above break time-reversal symmetry, as evident e.g., from the chosen directionality of the orbital motion of the Cooper pairs.

Even though the above homogeneous superconducting condensates spontaneously break time-reversal symmetry, their unambiguous detection in actual materials is challenging experimentally since the internal magnetic fields produced in these states are suppressed due to the condensate of overlapping Cooper pairs and Meissner screening. However, defects, edges, dislocations, twin boundary interfaces, and other spatial inhomogeneities are known to produce persistent current patterns with associated magnetic fields that do not average to zero [47–53, 57, 58, 79–86]. In Figure 2 we show several examples of disorder- and dislocation-induced current patterns in TRSB superconducting phases. The examples include cases where the homogeneous superconducting phase breaks time-reversal symmetry (Figure 2A, B), and a case (Figure 2C) where TRSB is only induced locally due to the dislocation, whereas the clean homogeneous superconducting phase preserves time-reversal symmetry, see also Ref. [87]. Naturally, a remaining important question is whether

FIGURE 3
(A) Zn impurity on 1D inorganic chain YBa_2NiO_5 [96]. NMR satellite lines (left) indicate different Ni nuclei at different distances from the Zn. Polarization (right) on each site oscillates in sign with distance [88]; **(B)** Elastic neutron scattering data on underdoped LSCO showing the intensity at the incommensurate Bragg peaks near (π, π) vs. temperature T [97]. While a magnetic field induces SDW order, significant incommensurate magnetism is present already in zero field. This effect is enhanced with Zn substitution [98]; **(C)** Highly anisotropic electronic states induced by strain near a NaFeAs grain boundary, interpreted as magnetic stripes along the Fe-Fe directions (blue arrows) [99]. **(A)** Reprinted figure with permission from [88], Copyright 2009 by the American Physical Society. **(B)** Reprinted figure with permission from [97], Copyright 2008 by the American Physical Society. **(C)** Reprinted from [99].

induced fields from this mechanism exhibit the required amplitudes and are voluminous enough to explain experiments of specific materials, or one needs to resort to other explanations for the TRSB signal. We return to this discussion in the final section of the paper.

2.2 Disorder and superconductivity-induced quasi-ordered magnetism
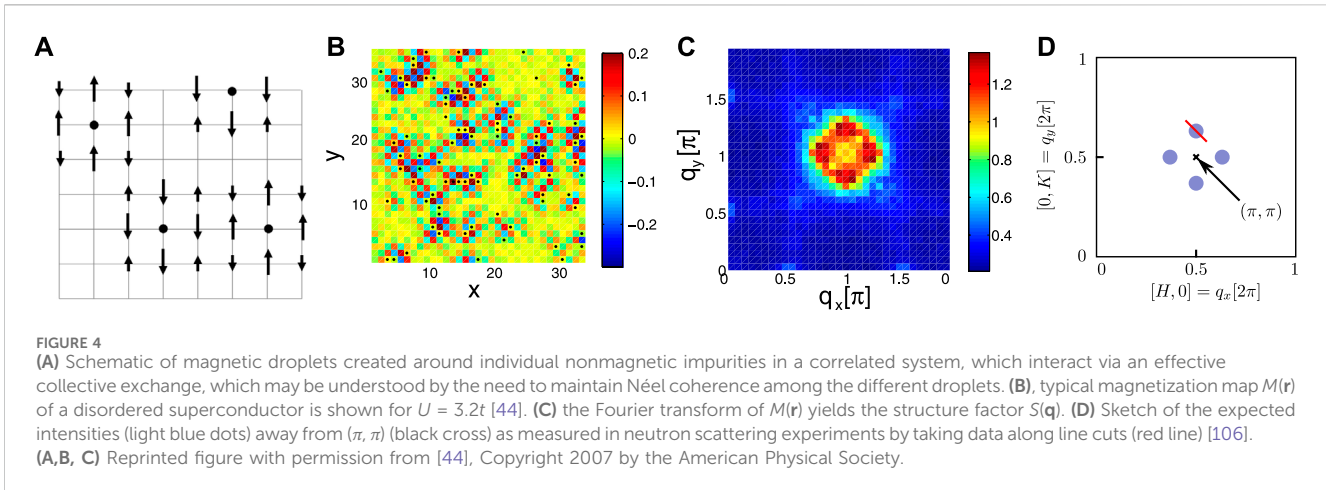
2.2.1 Magnetic droplets from impurities

Nonmagnetic disorder has been known for many years to give rise to magnetic bound states and magnetic glassy behavior in correlated electron systems [88]. In superconductors, the opening up of a gap promotes the existence of these bound states. For fixed correlation and gap size, increasing disorder "freezes" the spin fluctuations present in the system [46], transferring the spectral weight to low frequencies and creating static configurations of localized spins that can break time-reversal symmetry. There are several models that exhibit these phenomena in a qualitative sense, and many somewhat mysterious aspects of the phenomenology of underdoped cuprates can be explained on this basis [88]. The approach has been to begin with the study of simple, localized and isolated defects in model Fermi systems with strong antiferromagnetic correlations, like Hubbard, $t - J$, and Anderson models, combined as needed with BCS pairing interactions [40–45, 89–92]. The magnetic response generally takes the form of a "droplet" of magnetic correlations around a defect, whose effective size corresponds to the antiferromagnetic correlation length ξ_{AF} of the pure host. If the correlations and/or defect potentials are sufficiently strong, this droplet is spontaneously nucleated, carries net spin 1/2 and may be considered as a localized moment, but also displays a staggered magnetic behavior over ξ_{AF} [40–45]. If correlations or the impurity potential are weaker, the correlated spin response is still present, but must be induced by an applied magnetic field [45, 93]. This is a mean-field picture of the freezing of spin fluctuations present in the host, which needs to be supplemented by a description of dynamics, a complete version of which is still lacking. In the quantum critical regime, some aspects simplify, and the basic qualitative features have been discussed in Refs. [94, 95].

Away from the quantum critical point, the droplet picture has been extensively confirmed for dilute, intentionally substituted defects, primarily by NMR and μSR experiments in quasi-1D inorganic chain and ladder compounds (see Figure 3A) [96], as well as in some quasi-2D cuprate materials where impurity substitution into quite clean hosts can be adequately controlled [88]. On the other hand, there is no reason why similar physics should not take place when defects occur naturally in the crystal or film growth process, which is characteristic of many complex oxides, particularly chemically doped ones. The question then naturally arises as to what happens when the inter-defect spacing becomes comparable to the AF correlation length ξ_{AF}. In calculations for a 2D Hubbard model with disorder and d-wave pairing correlations, the overlap of the magnetic droplets in the correlated state leads to interference processes which tend to align the droplets in a state which displays quasi-long range AF order [44, 46, 100–102]. It seems likely that the results of many experiments which are attributed to "stripe order" in underdoped cuprates may in fact be explained by the quasi-long range order arising from interacting droplets [89, 103]. The creation of 1D structures to lower the kinetic energy via 1D rivers of mobile charge while maintaining some correlation energy is clearly an attractive and simple picture. But creation of such structures also raises the energy of the state around a single impurity, which would prefer to be more globular in shape. One can, within Hubbard-type models on square lattices, answer the question about which mechanism enables the system to lower its energy more efficiently in which situation. This clearly depends on a variety of factors, including doping, correlations, and disorder. By performing simulations, one can - without prejudicing the system - determine which part of the generalized phase diagram corresponds to 1D stripe-like structures, and which to other ground states [89, 104, 105].

Experimentally, manifestations of this physics have been observed in a wide variety of contexts. In Figure 3A, we show the well-established oscillations in the Y NMR line in a 1D inorganic chain due to the modulation of the magnetic response locally by a Zn
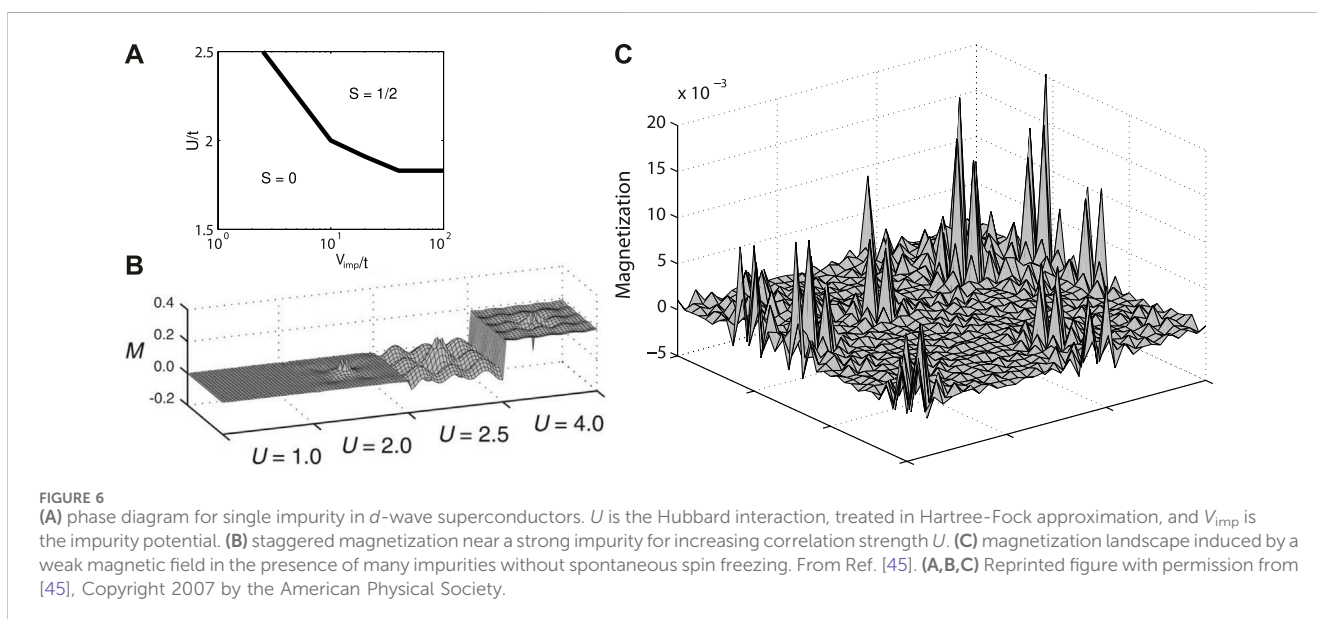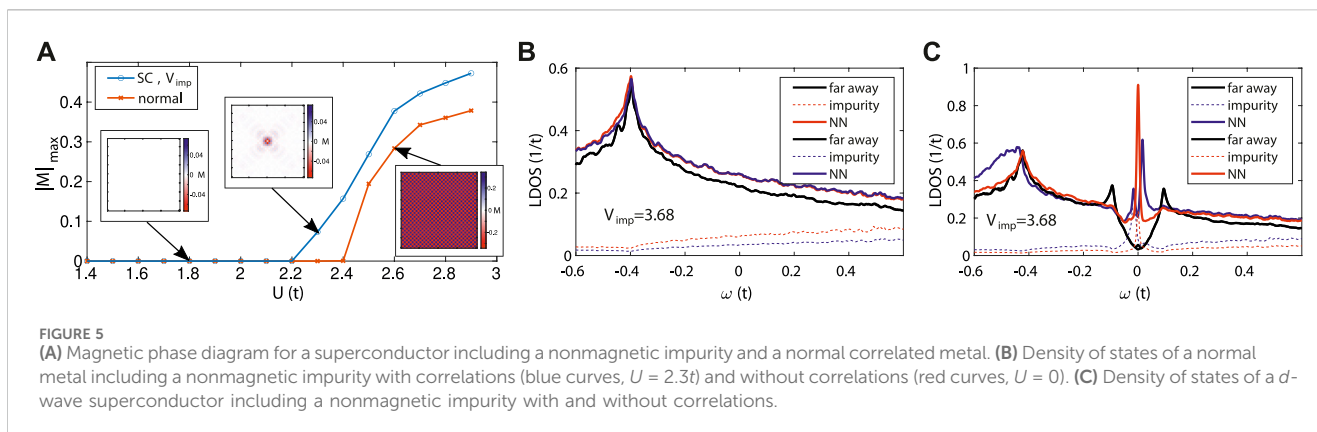
FIGURE 4
(A) Schematic of magnetic droplets created around individual nonmagnetic impurities in a correlated system, which interact via an effective collective exchange, which may be understood by the need to maintain Néel coherence among the different droplets. **(B)**, typical magnetization map $M(\mathbf{r})$ of a disordered superconductor is shown for $U = 3.2t$ [44]. **(C)** the Fourier transform of $M(\mathbf{r})$ yields the structure factor $S(\mathbf{q})$. **(D)** Sketch of the expected intensities (light blue dots) away from (π, π) (black cross) as measured in neutron scattering experiments by taking data along line cuts (red line) [106]. **(A,B, C)** Reprinted figure with permission from [44], Copyright 2007 by the American Physical Society.

impurity. Figure 3B shows data from an elastic neutron study [97] (see also [106–108]) with frozen magnetic order in a disordered cuprate in zero field, enhanced further by application of a field. The order is apparently quasi-long-ranged since it appears in the neutron scattering intensity near wave vector (π, π), yet it occurs in a part of the cuprate phase diagram where true long-range order has disappeared. Finally, in Figure 3C, STM reveals in an Fe-based superconductor a spatially modulated density of states pattern due to strain near a twin boundary with a wave vector close the $(\pi, 0)$ magnetic ordering vector, indicating local impurity-induced magnetism.

2.2.2 Quasi-long range magnetic order from disorder

Quasi long-range antiferromagnetic order has been reported in many cuprate samples whose T_c or nominal doping puts them outside the long-range AF phase, particularly in the superconducting state at low temperatures, e.g., in LSCO [97, 98, 106, 107, 109–112]. Characteristic dynamical features of spin glasses have occasionally been observed, but even if these are not always found, the term "spin glass" has become commonplace in cuprates to describe the existence of a phase of short-range frozen magnetism. The size of the spin-glass phase varies significantly with material [112]; whereas in LSCO it extends in zero field out to 15% doping, it is confined to very low doping in the much cleaner YBCO system [113, 114], and BSCCO is in-between [112]. Moreover, disorder due to Zn substitution on the Cu sites enhances the size of the spin-glass phase [98]. These empirical facts suggest strongly the picture of disorder-induced short-range magnetism described above. Quasi-long range order occurs when these droplets begin to overlap [44], which can occur without frustration on a square lattice, as shown in Figure 4A. This lack of frustration has important implications not only for the quasi-long range (π, π) magnetic order, but may also carry a macroscopic net magnetic moment. Since each droplet of *staggered* order is dominated by the NN spins, it carries a net spin 1/2 [41], and the droplets overlap coherently. While the net moments associated with each droplet do not align ferromagnetically, a fluctuating magnetic state with both short range and longer range (inter-impurity distance) is created

(Figure 4B). The final magnetization profile appears as a clear peak in the structure factor, as seen in Figure 4C, compared to the Lake et al. experiment on underdoped LSCO where intensity at the incommensurate positions is found [106], as shown schematically in Figure 4D. It is this disorder-induced random magnetic landscape that is relevant to our current study as a possible mechanism of TRSB in superconductors.

Thus far we have said little about why such a TRSB signal might arise only below T_c, as observed in many unconventional superconductors. Here the proposal is that the gapping of the low-energy density of states enhances the probability of creating an impurity bound state carrying the spin-1/2 moment. Figure 5A shows the selfconsistently obtained magnetization in the presence of a nonmagnetic point-like impurity at $T = 0$ *versus* Hubbard U. As seen, before entering the bulk SDW phase, a regime exists where the superconductor prefers a local impurity-induced magnetic droplet as discussed above. What is the origin of this local magnetic structure? In Figure 5B, we show the local density of states of the tight-binding model with band parameters suitable for a cuprate superconductor. Addition of a strong impurity does not produce a bound state resonance due to the fact that the impurity state is embedded in the continuum. Addition of correlations does not change this qualitative picture. On the other hand, when a superconducting gap is created, as in the d-wave case shown in Figure 5C, the expected in-gap resonance is clearly visible (compare, e.g., with Zn impurity in BSCCO [115]). In the presence of correlations, the bound state splits to lower the overall energy including magnetism, creating in the process the localized spin-1/2 state with maximal polarization typically on nearest neighbor sites. Creating such a state depends both on the impurity potential V_{imp} and on the strength of the correlations U, as shown in the "phase diagram" of Figure 6A. The explicit evolution of the 1-impurity local magnetic state for increasing correlation strength is shown in Figure 6B: it is stabilized in a range of U just below the critical U corresponding to creation of true long-range order in the Hartree-Fock approximation. Even if the magnetic bound states are not formed spontaneously, i.e., one is in the $S = 0$ part of the phase diagram shown in 6 A, it is important to recall that the system is still highly correlated as indicated by the response of many impurities for small but nonzero U to a weak magnetic field, as seen from Figure 6C.

FIGURE 5
(A) Magnetic phase diagram for a superconductor including a nonmagnetic impurity and a normal correlated metal. **(B)** Density of states of a normal metal including a nonmagnetic impurity with correlations (blue curves, $U = 2.3t$) and without correlations (red curves, $U = 0$). **(C)** Density of states of a d-wave superconductor including a nonmagnetic impurity with and without correlations.

FIGURE 6
(A) phase diagram for single impurity in d-wave superconductors. U is the Hubbard interaction, treated in Hartree–Fock approximation, and V_{imp} is the impurity potential. **(B)** staggered magnetization near a strong impurity for increasing correlation strength U. **(C)** magnetization landscape induced by a weak magnetic field in the presence of many impurities without spontaneous spin freezing. From Ref. [45]. **(A,B,C)** Reprinted figure with permission from [45], Copyright 2007 by the American Physical Society.

Similar phenomena have been observed in many other correlated superconductors. Most recently, magnetic clustering was reported by μSR in samples of UTe$_2$ grown by chemical vapor transport with T_c's of order 1.6K [116], whereas no magnetic signal was reported in cleaner molten-salt flux grown crystals with T_c's of order 2.1K [117].

To summarize this section, simulations of a d-wave superconductor in the presence of local Coulomb interactions and nonmagnetic disorder [44, 89, 101, 103] are compatible with the experiments on relatively disordered cuprates like LSCO and BSCCO where a spin-glass phase is observed at low doping in the SC state [112]. These studies explain as well why such a phase is *not* seen in the cleanest YBCO samples, why in LSCO and BSCCO the spin-glass phase is more robust at underdoping, and why it is enhanced by addition of further disorder. The order-from-disorder many-impurity magnetic state is favored to appear only below T_c when the gap opens. Similar phenomena have been observed in other correlated superconductors [91, 118–120].

2.2.3 TRSB from disorder-induced loop currents

Recently, a Bogoliubov-de Gennes study of a disordered d-wave superconductor without magnetic correlations [55] reported local TRSB

current loops for sufficiently high disorder levels, see Figure 7A. Since a pure d-wave superconducting state does not break time-reversal symmetry, and parameters are chosen to place the pure system far from TRSB mixed-symmetry states ($d + is$), it is surprising that such persistent currents can arise purely from nonmagnetic disorder. In addition, the possible emergence of an effective granular d-wave description was proposed by Li et al. [55]. In this picture, cuprates consist of intrinsically inhomogeneous d-wave regions of roughly constant phase, weakly coupled by Josephson tunneling. For example, such behavior has been claimed experimentally from STM, magnetization and transport measurements on certain overdoped LSCO samples [121]. Such a proposal, if correct, would have profound implications for the disappearance of superconductivity on the overdoped side of the superconducting dome, since phase fluctuations, rather than pair interaction weakening (as due, for example, to the weakening of spin fluctuations and disorder [122]) would determine T_c.

However, detailed theoretical investigations of the disorder-induced orbital currents in the same model framework were performed in Ref. [56], showing that the occurrence of such currents can be traced to local extended s-wave pairing out of

FIGURE 7
(A) Spontaneous current pattern in a d-wave superconductor with large disorder [55]. **(B)** Zero temperature phase diagram indicating average current (red triangles, left scale) vs. doping. Also indicated are s- and d-wave order parameter amplitudes, respectively (solid lines). The shaded region marks the range of doping where a mixed state $s + id$ is stable in the homogeneous case. Dashed lines show the average d-wave (purple) and s-wave (green) order parameter components (see main text) with random distributions of impurities [56]. **(A)** Reproduced from [55]. CC BY 4.0. **(B)** Reprinted figure with permission from [56], Copyright 2007 by the American Physical S.ociety.

phase with d-wave order, despite the fact that the effect occurs far from the homogeneous $s + id$ phase (see Figure 7B). The system does not appear to spontaneously phase separate into granular regions. Instead, the energetics leading to regions of *local $s \pm id$* order are driven by inhomogeneous density modulations.

2.3 Enhanced RKKY exchange coupling and slowing-down of magnetic fluctuations by superconductivity

While the previous sections addressed the case where superconductivity is a necessary ingredient for orbital currents or moment formation, here we focus on different scenarios where disorder and superconductivity interact to either slow down magnetic fluctuations or enhance the mutual coupling between magnetic regions/moments existing already in the normal state. This section serves to suggest alternative mechanisms for observing TRSB below T_c. We focus on the physical picture and outline several options whereas a quantitative study is left for future research. We consider the following possibilities:

- (A) Time-reversal symmetry is preserved in the normal state, but disorder pins or slows down fluctuations in the superconducting state to either break time-reversal symmetry or bring the system closer to local magnetism.
- (B) The normal state contains significant amounts of magnetic moments, but time-reversal symmetry remains preserved in the normal state. The magnetic moments get resonantly coupled in the superconducting state thereby breaking time-reversal symmetry or bringing the system closer to static magnetism.
- (C) Time-reversal symmetry is broken already in the normal state, yet too weak or dilute to be detected by standard

experimental probes. Superconductivity enhances the magnetic volume fraction and/or increases the coupling between magnetic regions.

The first **scenario (A)** was largely discussed in Sec. 2.2, there exemplified through models relevant for cuprates, i.e., $d_{x^2-y^2}$-wave superconductivity in the presence of nonmagnetic impurities and electronic correlations. This mechanism is likely much more broadly applicable since most unconventional superconductors allow for in-gap bound states from nonmagnetic disorder [90, 123, 124]. This causes enhanced local spin susceptibilities and associated tendency to slow down magnetic fluctuations locally or even pin magnetic moments [88]. This mechanism may well also be at play near e.g., sample edges or various forms of dislocations [57, 58, 125, 126]. A related property may happen near sample edges when zero-energy Andreev bound states generated by sign-changes of the gap function split by spontaneous generation of edge supercurrents [82, 84, 86].

Regarding **scenario (B)**, consider the case of a normal metal with a concentration of magnetic moments. Due to quantum fluctuations, time-reversal symmetry is preserved in the normal state. We assume additionally a low Kondo temperature, $T_K < T_c$, i.e., unscreened spins. We return briefly to the opposite case with $T_K > T_c$ further below. The magnetic moments couple via the indirect Ruderman-Kittel-Kasuya-Yosida (RKKY) interaction, i.e., via a partial spin polarization of the conduction electrons, causing the well-known oscillatory RKKY exchange interaction [127–129]. The detailed behavior of the RKKY coupling in the superconducting phase depends on dimensionality, the normal state bandstructure, and the superconducting pairing symmetry, and is generally a complex matter that requires thorough investigation [130–133]. Typically, however, for spin-singlet superconductivity the RKKY coupling is weakened by the singlet formation of the conduction electrons. More specifically, for the standard RKKY interaction s-wave superconductivity contributes a weak

antiferromagnetic correction when the inter-moment distance R is smaller than the coherence length ξ. For $R > \xi$, the RKKY coupling becomes purely antiferromagnetic from the anomalous (superconducting) part of the spin susceptibility, but is exponentially suppressed in R [130]. These are consequences of the typical suppressed spin susceptibility in the superconducting phase. It is important to emphasize that these properties apply to the perturbative RKKY expression calculated in the Born approximation, only in the case of s-wave spin-singlet superconductivity.

It is known, however, that another contribution to the exchange coupling arises from the Yu-Shiba-Rusinov (YSR) bound states produced by magnetic impurities [123, 134–137]. The overlap of the YSR bound state wavefunctions leads to a resonant-like contribution to the energy with a singular dependence of the exchange coupling on the YSR bound state energy [137]. Thus, in some superconductors where the average distance between the magnetic moments is lower than ξ, it is conceivable (though somewhat fine-tuned due to the requirement of very low-lying YSR states [137, 138]) that the RKKY coupling gets enhanced in the superconducting phase, thereby boosting the tendency for magnetism and the detection of a TRSB signal only below T_c. In fact, this mechanism may also be at play for the mechanism discussed in Sec. 2.2 where magnetic moments are generated only by electronic interactions and superconducting bound states from nonmagnetic impurity potentials. To the best of our knowledge, the resonant-like YSR energy contribution has not been thoroughly investigated for other superconducting pairing symmetries, but presumably nodal gaps or triplet order can drive even stronger, directional-dependent couplings [131]. Quantum corrections to the classical YSR picture can also in principle lead to TRSB enhancement in the superconducting state, if in the case $T_K \gtrsim T_c$, spin-singlet superconducting gap formation unscreens the moments. In that case, if the moments couple and generate a weak magnetic state, it may be picked up by e.g., μSR similarly to the scenario discussed in Sec. 2.2.

Finally we discuss **scenario (C)** where a distribution of disordered static magnetic moments are already present in the normal state. Thus in this case, strictly speaking, TRSB is not restricted to the superconducting phase below Tc. We do not discuss in detail the origin of such moments, but they could simply arise from weakly coupled magnetic impurities, or small spin-polarized regions that have crossed into a nearby magnetic phase due to chemical disorder. It might also be due to the mechanism discussed in Sec. 2.2 if the "normal state" exhibits pseudo-gap behavior. We assume that the magnetism in the normal state is too weak to be detected by standard probes, for example, due to a tiny volume fraction and/or short-range nature. A TRSB signal may be detected, however, in cases where the volume fraction grows and/or the moments couple more strongly, and the magnetic quasi-order becomes longer ranged as a result upon entering the superconducting phase [139, 116]. The latter may arise from the mechanism discussed under (B). It might also take place via new "stepping stone" magnetic islands produced by nonmagnetic disorder in the superconducting state via the mechanism discussed in Sec. 2.2. An enhanced volume fraction can take place in cases

where another competing order is in the game. If local disorder-induced magnetism is limited by orbital order or a CDW phase, for example, then superconductivity may suppress these competing orders and thereby alleviate the magnetism. Clearly, these are merely possibilities for observing TRSB below T_c, and need further detailed investigations for specific materials.

3 Experimental consequences

In this section we discuss the main current experimental techniques to directly probe TRSB in superconductors, and mention subtleties in the interpretation of experimental results. Many unconventional superconductors are investigated using the muon spin relaxation (μSR) technique where a beam of spin-polarized muons with given energy is directed to the sample [140]. Muons are stopped in the material, implanted at preferred positions in the crystal structure and can be used to detect the magnetic field locally at their positions. Within the lifetime of the muons, their spins precess in the local field. Once the muon decays into a positron and two neutrinos, the direction of the magnetic moment fixes the probability distribution of emitted positrons. The counting rates of the latter in the forward and backward directions of the (original) polarization of the muon beam yield the asymmetry $A(t)$, which is recorded as a function of time.

The Fourier transform of $A(t)$ for measurements on superconductors in a finite field (in the vortex state) is directly related to the magnetic field distribution of the sample and can be used to deduce the temperature dependence of the penetration depth [140–142]. In a zero field experiment, the information about the field distribution is also contained in the asymmetry function, but typically full oscillations are not observed in superconductors because of the smallness of the internal field. Still, an increased relaxation as a function of temperature is taken as signature of the occurrence of an additional internal field that collectively depolarizes the implanted muons. Average fields that are static on the time scale of the muon decay can then be detected down to the scale of μT [140]. From the shape of the asymmetry $A(t)$ at low temperature (when there is evidence for TRSB), it is possible to estimate the average field by the reduction at largest measuring times. A quick initial reduction and no further deviation as a function of time are indications of few muons getting depolarized in a large field. By contrast, an initial weak difference of the depolarization rates that behaves quadratically in time indicates an almost uniform field distribution. Fitting to such behavior can give bounds on the fraction of the sample exhibiting TRSB. Such bounds may be further benchmarked against scanning SQUID microscopy measurement [6, 143, 144]. Depending on the initial energy of the muons, implantation happens on length scales of 10 nm–100 nm from the surface, such that the technique can be considered as bulk-like. By varying the initial energy of the muons, the stopping profiles allow deductions of the TRSB as function of distance from the surface [139]. The μSR technique has been used to claim TRSB in a number of superconductors; for a list see Ref. [3].

Knowledge from *ab initio* methods about the preferred position within the elementary cell where muons are implanted [145, 146] can facilitate the interpretation of the results, i.e., help decipher whether the positive charge of the muons might cause a perturbation large enough to self-generate a TRSB signal. In addition, the position of the stopping site and the associated form factor can be important for a quantitative description of the relaxation, e.g., in cases where the muon locations may feature enhanced or reduced field effects from purely geometric reasons. The typical magnitude of the internal field at the muon site for a generic interstitial position in the unit cell may be estimated; in the vicinity of local spin-1/2 droplets (Sec. 2.2) or impurity-induced localized orbital currents are of order 1 G [3, 147], which is of the same order as fields reported in experiments.

The second main probe of TRSB is the polar Kerr effect, where the polarization plane of light incident on a sample is rotated upon reflection. The classic example is reflection from a ferromagnetic surface, but in recent years the technique has been employed to detect TRSB in unconventional superconductors [1, 2, 148–151]. The angle θ_K, which is related to the Hall conductivity, can be expressed as

$$\theta_K(\omega) = \frac{4\pi}{\omega} \text{Im}\left(\frac{\sigma_H(\omega)}{n(n^2-1)}\right),$$

where n is the complex, frequency-dependent index of refraction, and $\sigma_H(\omega)$ is the Hall conductivity. For the experimental identification of a polar Kerr effect arising from the superconducting state, it needs to be checked that the rotation onsets at T_c, the sign and magnitude of the signals vary after each cool-down in the absence of an external magnetic field, a small training field saturates the rotation angle (but with sign given by the direction of the field), and the temperature dependence of the Kerr angle follows mean-field-like order parameter behavior [148].

From a theoretical point of view, a finite Kerr angle is directly related to a nonzero Hall conductivity, which requires time-reversal symmetry breaking and breaking of mirror symmetries about all planes parallel to the incident wave vector [152]. Therefore, the order parameter has to be chiral and not simply break TRSB. For example, a pure $s + id$ superconductor is nonchiral and will not generate an intrinsic Kerr signal. By contrast, a one-band $p + ip$ superconductor will produce a weak intrinsic Kerr effect with θ_K arising only from the collective modes of the order parameter [153]. This effect is many orders of magnitude smaller than typical measured rotation angles θ_K of order tens of nanoradians. The intrinsic effect in a chiral *multiband* superconductor, arising from contributions to σ_H from interband transitions, is larger at optical frequencies (but still difficult to definitively quantify) [154]. On the other hand, if the state is nonchiral, there will be no intrinsic Kerr signal at all.

It is important to note that chirality can occur for complex linear combinations of 1D irreps of the point group, and not necessarily only those states corresponding to 2D irreps that have been traditionally discussed, like $p_x + ip_y$ in tetragonal and $d_{xy} + id_{x^2-y^2}$ in hexagonal symmetries. For example, in tetragonal symmetry, $d_{x^2-y^2}$ and d_{xy} are distinct 1D irreps, but may occur in an accidental linear combination $a \cdot d_{xy} + ib \cdot d_{x^2-y^2}$. Such states should also give rise to an intrinsic polar Kerr effect, but nonchiral TRSB combinations like $s + id$ will not.

One of the problems with the interpretation of Kerr measurements is that the size of an intrinsic signal is very hard to estimate, and the size of an extrinsic one may in principle be in fact much larger, but depend on the type of disorder and the nature of the ground state. For example, the division between chiral and non-chiral states with regard to their polar Kerr signals is muddied somewhat by disorder. In $p + ip$ states, an extrinsic Kerr rotation angle orders of magnitude larger than the intrinsic effect may result from the skew-scattering of chiral Cooper pairs from impurities [155, 156], but for $d + id$ and higher order angular momentum states, the contribution is of higher order in (nV_{imp}^2) where V_{imp} is the impurity potential of point-like impurities with density n [1, 155]. Estimates in both cases are model dependent and require disorder averaging. Impurities in nonchiral TRSB states will also give rise to small signals from induced currents, but after averaging such signals should be substantially smaller, while for chiral $d + id$ states the signal is small but remains finite upon impurity averaging [157]. A similar contribution should therefore be provided by local spatially fluctuating magnetic moments. Whether or not a Kerr signal is observed, and its size, depends on how much averaging of the fluctuations takes place over the laser spot. In both these cases, some kind of ability to "train" the state with an external magnetic field should be observed [148]. Finally, we mention some recent calculations showing that local currents can be created near dislocations, which induce $d + ig$ or $s + id$ states [57, 58]. The Kerr effect arising from these local states has not been properly explored.

4 Summary and outlook

In the above we focused on different theoretical mechanisms where magnetism in various guises appear only below the superconducting critical transition temperature T_c and is generated by disorder or other spatial inhomogeneities. This included discussions of localized defect-induced orbital supercurrents, magnetic moment generation from superconductivity and electronic correlations, and the possibility of enhanced RKKY exchange coupling by superconductivity.

Naturally an important question relates to the relevance of these mechanisms to the observation of TRSB below T_c in currently discussed unconventional superconducting materials. In the above, we provided a detailed discussion of the cuprates and the possibility of superconductivity-enhanced spin-polarization. Two other materials of significant current interest are UTe$_2$ and Sr$_2$RuO$_4$. For these compounds, two-component condensates are widely discussed, but inconsistent with specific heat measurements, also under uniaxial strain featuring no signs of double transitions [36–39]. This points to single-component superconductivity which has received recent support from a number of other probes as well [117, 150, 158, 159], but leaves open the question of what causes a TRSB signal in some measurements. We have surveyed several possible answers to this question from the perspective of induced fields within the superconducting state from spatial inhomogeneity.

Resolving the detailed nature of TRSB in superconductors is important since the resolution will have profound implications for our general understanding of unconventional superconductivity. Therefore, we hope that future collective research efforts will

continue to be devoted to this task. This includes both improved experiments and better theoretical descriptions, the latter including material-specific studies of the interplay between unconventional pairing states and realistic models for the relevant sources of spatial inhomogeneity. μSR and Kerr experiments on systematically disordered samples, e.g., with strong chemical impurities or Frenkel defects created by electron irradiation, can help to distinguish the extrinsic TRSB effects described here from intrinsic effects, and from each other.

Author contributions

BA: Writing–original draft. AK: Writing–original draft. PH: Writing–original draft.

Funding

Acknowledgments

Conflict of interest

The authors declare that the research was conducted in the absence of any commercial or financial relationships that could be construed as a potential conflict of interest.

Publisher's note

All claims expressed in this article are solely those of the authors and do not necessarily represent those of their affiliated organizations, or those of the publisher, the editors and the reviewers. Any product that may be evaluated in this article, or claim that may be made by its manufacturer, is not guaranteed or endorsed by the publisher.

References

1. Kallin C, Berlinsky J. Chiral superconductors. *Rep Prog Phys* (2016) 79:054502. doi:10.1088/0034-4885/79/5/054502

2. Wysokiński KI. Time reversal symmetry breaking superconductors: Sr_2RuO_4 and beyond. *Condensed Matter* (2019) 4:47. doi:10.3390/condmat4020047

3. Ghosh SK, Smidman M, Shang T, Annett JF, Hillier AD, Quintanilla J, et al. Recent progress on superconductors with time-reversal symmetry breaking. *J Phys Condens Matter* (2021) 33:033001. doi:10.1088/1361-648x/abaa06

4. Røising HS, Wagner G, Roig M, Rømer AT, Andersen BM. Heat capacity double transitions in time-reversal symmetry broken superconductors. *Phys Rev B* (2022) 106: 174518. doi:10.1103/PhysRevB.106.174518

5. Strand JD, Van Harlingen DJ, Kycia JB, Halperin WP. Evidence for complex superconducting order parameter symmetry in the low-temperature phase of UPt_3 from Josephson interferometry. *Phys Rev Lett* (2009) 103:197002. doi:10.1103/PhysRevLett.103.197002

6. Hicks CW, Kirtley JR, Lippman TM, Koshnick NC, Huber ME, Maeno Y, et al. Limits on superconductivity-related magnetization in Sr_2RuO_4 and $PrOs_4Sb_{12}$ from scanning SQUID microscopy. *Phys Rev B* (2010) 81:214501. doi:10.1103/PhysRevB.81.214501

7. Avers KE, Gannon WJ, Kuhn SJ, Halperin WP, Sauls JA, DeBeer-Schmitt L, et al. Broken time-reversal symmetry in the topological superconductor UPt_3. *Nat Phys* (2020) 16:531–5. doi:10.1038/s41567-020-0822-z

8. Maeno Y, Hashimoto H, Yoshida K, Nishizaki S, Fujita T, Bednorz JG, et al. Superconductivity in a layered perovskite without copper. *Nature (London)* (1994) 372: 532–4. doi:10.1038/372532a0

9. Mackenzie AP, Scaffidi T, Hicks CW, Maeno Y. Even odder after twenty-three years: the superconducting order parameter puzzle of Sr_2RuO_4. *Npj Quan Mater.* (2017) 2:40. doi:10.1038/s41535-017-0045-4

10. Rømer AT, Scherer DD, Eremin IM, Hirschfeld PJ, Andersen BM. Knight shift and leading superconducting instability from spin fluctuations in Sr_2RuO_4. *Phys Rev Lett* (2019) 123:247001. doi:10.1103/PhysRevLett.123.247001

11. Rømer AT, Hirschfeld PJ, Andersen BM. Superconducting state of Sr_2RuO_4 in the presence of longer-range Coulomb interactions. *Phys Rev B* (2021) 104:064507. doi:10.1103/PhysRevB.104.064507

12. Kivelson SA, Yuan AC, Ramshaw BJ, Thomale R. A proposal for reconciling diverse experiments on the superconducting state in Sr_2RuO_4. *Npj Quan Mater.* (2020) 5:43. doi:10.1038/s41535-020-0245-1

13. Stewart GR. Heavy-fermion systems. *Rev Mod Phys* (1984) 56:755–87. doi:10.1103/RevModPhys.56.755

14. Joynt R, Taillefer L. The superconducting phases of UPt_3. *Rev Mod Phys* (2002) 74: 235–94. doi:10.1103/RevModPhys.74.235

15. Kawasaki I, Watanabe I, Hillier A, Aoki D. Time-reversal symmetry in the hidden order and superconducting states of URu_2Si_2. *J Phys Soc Jpn* (2014) 83:094720. doi:10.7566/JPSJ.83.094720

16. Ran S, Eckberg C, Ding QP, Furukawa Y, Metz T, Saha SR, et al. Nearly ferromagnetic spin-triplet superconductivity. *Science* (2019) 365:684–7. doi:10.1126/science.aav8645

17. Aoki D, Brison JP, Flouquet J, Ishida K, Knebel G, Tokunaga Y, et al. Unconventional superconductivity in UTe_2. *J Phys Condens Matter* (2022) 34: 243002. doi:10.1088/1361-648x/ac5863

18. Biswas PK, Luetkens H, Neupert T, Stürzer T, Baines C, Pascua G, et al. Evidence for superconductivity with broken time-reversal symmetry in locally noncentrosymmetric SrPtAs. *Phys Rev B* (2013) 87:180503. doi:10.1103/PhysRevB.87.180503

19. Shang T, Smidman M, Ghosh SK, Baines C, Chang LJ, Gawryluk DJ, et al. Time-reversal symmetry breaking in Re-based superconductors. *Phys Rev Lett* (2018) 121: 257002. doi:10.1103/PhysRevLett.121.257002

20. Shang T, Ghosh SK, Zhao JZ, Chang LJ, Baines C, Lee MK, et al. Time-reversal symmetry breaking in the noncentrosymmetric Zr_3Ir superconductor. *Phys Rev B* (2020) 102:020503. doi:10.1103/PhysRevB.102.020503

21. Hillier AD, Quintanilla J, Cywinski R. Evidence for time-reversal symmetry breaking in the noncentrosymmetric superconductor $LaNiC_2$. *Phys Rev Lett* (2009) 102: 117007. doi:10.1103/PhysRevLett.102.117007

22. Hillier AD, Quintanilla J, Mazidian B, Annett JF, Cywinski R. Nonunitary triplet pairing in the centrosymmetric superconductor $LaNiGa_2$. *Phys Rev Lett* (2012) 109: 097001. doi:10.1103/PhysRevLett.109.097001

23. Bauer ED, Frederick NA, Ho PC, Zapf VS, Maple MB. Superconductivity and heavy fermion behavior in $PrOs_4Sb_{12}$. *Phys Rev B* (2002) 65:100506. doi:10.1103/PhysRevB.65.100506

24. Aoki Y, Tsuchiya A, Kanayama T, Saha SR, Sugawara H, Sato H, et al. Time-reversal symmetry-breaking superconductivity in heavy-fermion $PrOs_4Sb_{12}$ detected by muon-spin relaxation. *Phys Rev Lett* (2003) 91:067003. doi:10.1103/PhysRevLett.91.067003

25. Rotter M, Tegel M, Johrendt D. Superconductivity at 38 K in the iron arsenide $(Ba_{1-x}K_x)Fe_2As_2$. *Phys Rev Lett* (2008) 101:107006. doi:10.1103/PhysRevLett.101.107006

26. Böker J, Volkov PA, Efetov KB, Eremin I. $s + is$ superconductivity with incipient bands: doping dependence and STM signatures. *Phys Rev B* (2017) 96:014517. doi:10.1103/PhysRevB.96.014517

27. Matsuura K, Roppongi M, Qiu M, Sheng Q, Cai Y, Yamakawa K, et al. Two superconducting states with broken time-reversal symmetry in $FeSe_{1-x}S_x$. *Proc Natl Acad Sci* (2023) 120:e2208276120. doi:10.1073/pnas.2208276120

28. Guguchia Z, Mielke C, Das D, Gupta R, Yin JX, Liu H, et al. Tunable unconventional kagome superconductivity in charge ordered RbV_3Sb_5 and KV_3Sb_5. *Nat Commun* (2023) 14:153. doi:10.1038/s41467-022-35718-z

29. Mielke C, Das D, Yin JX, Liu H, Gupta R, Jiang YX, et al. Time-reversal symmetry-breaking charge order in a kagome superconductor. *Nature* (2022) 602:245–50. doi:10.1038/s41586-021-04327-z

30. Rømer AT, Bhattacharyya S, Valenti R, Christensen MH, Andersen BM. Superconductivity from repulsive interactions on the kagome lattice. *Phys Rev B* (2022) 106:174514. doi:10.1103/PhysRevB.106.174514

31. Ribak A, Skiff RM, Mograbi M, Rout PK, Fischer MH, Ruhman J, et al. Chiral superconductivity in the alternate stacking compound 4Hb-TaS_2. *Sci Adv* (2020) 6: eaax9480. doi:10.1126/sciadv.aax9480

32. Anand VK, Bhattacharyya A, Adroja DT, Panda K, Biswas PK, Hillier AD, et al. Time-reversal symmetry breaking and s-wave superconductivity in $CaPd_2Ge_2$: a μSR study. *Phys Rev B* (2023) 108:224519. doi:10.1103/PhysRevB.108.224519

33. Kataria A, Verezhak JAT, Prakash O, Kushwaha RK, Thamizhavel A, Ramakrishnan S, et al. Time-reversal symmetry breaking in the superconducting low carrier density quasiskutterudite $Lu_3Os_4Ge_{13}$. *Phys Rev B* (2023) 107:L100506. doi:10.1103/PhysRevB.107.L100506

34. Kataria A, Verezhak JAT, Prakash O, Kushwaha RK, Thamizhavel A, Ramakrishnan S, et al. Broken time-reversal symmetry in the cubic skutterudite-like superconductor $Y_3Ru_4Ge_{13}$. *Phys Rev B* (2023) 108:214512. doi:10.1103/PhysRevB.108.214512

35. Bhattacharyya A, Adroja D, Feng Y, Das D, Biswas PK, Das T, et al. μSR study of unconventional pairing symmetry in the quasi-1D $Na_2Cr_3As_3$ superconductor. *Magnetochemistry* (2023) 9:70. doi:10.3390/magnetochemistry9030070

36. Steppke A, Zhao L, Barber ME, Scaffidi T, Jerzembeck F, Rosner H, et al. Strong peak in T_c of Sr_2RuO_4 under uniaxial pressure. *Science* (2017) 355:eaaf9398. doi:10.1126/science.aaf9398

37. Li YS, Kikugawa N, Sokolov DA, Jerzembeck F, Gibbs AS, Maeno Y, et al. High-sensitivity heat-capacity measurements on Sr_2RuO_4 under uniaxial pressure. *Proc Natl Acad Sci USA* (2021) 118:e2020492118. doi:10.1073/pnas.2020492118

38. Rosa PFS, Weiland A, Fender SS, Scott BL, Ronning F, Thompson JD, et al. Single thermodynamic transition at 2 K in superconducting UTe_2 single crystals. *Commun Mater* (2022) 3:33. doi:10.1038/s43246-022-00254-2

39. Girod C, Stevens CR, Huxley A, Bauer ED, Santos FB, Thompson JD, et al. Thermodynamic and electrical transport properties of UTe_2 under uniaxial stress. *Phys Rev B* (2022) 106:L121101. doi:10.1103/PhysRevB.106.L121101

40. Tsuchiura H, Tanaka Y, Ogata M, Kashiwaya S. Local magnetic moments around a nonmagnetic impurity in the two-dimensional $t − J$ model. *Phys Rev B* (2001) 64: 140501. doi:10.1103/PhysRevB.64.140501

41. Wang Z, Lee PA. Local moment formation in the superconducting state of a doped Mott insulator. *Phys Rev Lett* (2002) 89:217002. doi:10.1103/PhysRevLett.89.217002

42. Zhu JX, Martin I, Bishop AR. Spin and charge order around vortices and impurities in high-T_c superconductors. *Phys Rev Lett* (2002) 89:067003. doi:10.1103/PhysRevLett.89.067003

43. Chen Y, Ting CS. States of local moment induced by nonmagnetic impurities in cuprate superconductors. *Phys Rev Lett* (2004) 92:077203. doi:10.1103/PhysRevLett.92.077203

44. Andersen BM, Hirschfeld PJ, Kampf AP, Schmid M. Disorder-induced static antiferromagnetism in cuprate superconductors. *Phys Rev Lett* (2007) 99:147002. doi:10.1103/PhysRevLett.99.147002

45. Harter JW, Andersen BM, Bobroff J, Gabay M, Hirschfeld PJ. Antiferromagnetic correlations and impurity broadening of NMR linewidths in cuprate superconductors. *Phys Rev B* (2007) 75:054520. doi:10.1103/PhysRevB.75.054520

46. Andersen BM, Graser S, Hirschfeld PJ. Disorder-induced freezing of dynamical spin fluctuations in underdoped cuprate superconductors. *Phys Rev Lett* (2010) 105: 147002. doi:10.1103/PhysRevLett.105.147002

47. Lee WC, Zhang SC, Wu C. Pairing state with a time-reversal symmetry breaking in FeAs-based superconductors. *Phys Rev Lett* (2009) 102:217002. doi:10.1103/PhysRevLett.102.217002

48. Garaud J, Babaev E. Domain walls and their experimental signatures in $s + is$ superconductors. *Phys Rev Lett* (2014) 112:017003. doi:10.1103/PhysRevLett.112.017003

49. Maiti S, Sigrist M, Chubukov A. Spontaneous currents in a superconductor with $s + is$ symmetry. *Phys Rev B* (2015) 91:161102. doi:10.1103/PhysRevB.91.161102

50. Lin SZ, Maiti S, Chubukov A. Distinguishing between $s + id$ and $s + is$ pairing symmetries in multiband superconductors through spontaneous magnetization pattern induced by a defect. *Phys Rev B* (2016) 94:064519. doi:10.1103/PhysRevB.94.064519

51. Garaud J, Silaev M, Babaev E. Thermoelectric signatures of time-reversal symmetry breaking states in multiband superconductors. *Phys Rev Lett* (2016) 116: 097002. doi:10.1103/PhysRevLett.116.097002

52. Benfenati A, Barkman M, Winyard T, Wormald A, Speight M, Babaev E. Magnetic signatures of domain walls in $s + is$ and $s + id$ superconductors: observability and what that can tell us about the superconducting order parameter. *Phys Rev B* (2020) 101: 054507. doi:10.1103/PhysRevB.101.054507

53. Roig M, Rømer AT, Hirschfeld PJ, Andersen BM. Revisiting superconductivity in the extended one-band Hubbard model: pairing via spin and charge fluctuations. *Phys Rev B* (2022) 106:214530. doi:10.1103/PhysRevB.106.214530

54. Yerin Y, Drechsler SL, Cuoco M, Petrillo C. Magneto-topological transitions in multicomponent superconductors. *Phys Rev B* (2022) 106:054517. doi:10.1103/PhysRevB.106.054517

55. Li ZX, Kivelson SA, Lee DH. Superconductor-to-metal transition in overdoped cuprates. *npj Quan Mater* (2021) 6:36. doi:10.1038/s41535-021-00335-4

56. Breiø CN, Hirschfeld PJ, Andersen BM. Supercurrents and spontaneous time-reversal symmetry breaking by nonmagnetic disorder in unconventional superconductors. *Phys Rev B* (2022) 105:014504. doi:10.1103/PhysRevB.105.014504

57. Willa R, Hecker M, Fernandes RM, Schmalian J. Inhomogeneous time-reversal symmetry breaking in Sr_2RuO_4. *Phys Rev B* (2021) 104:024511. doi:10.1103/PhysRevB.104.024511

58. Breiø CN, Kreisel A, Roig M, Hirschfeld PJ, Andersen BM. Time-reversal symmetry breaking from lattice dislocations in superconductors. *Phys Rev B* (2024) 109:014505. doi:10.1103/PhysRevB.109.014505

59. Ying YA, Staley NE, Xin Y, Sun K, Cai X, Fobes D, et al. Enhanced spin-triplet superconductivity near dislocations in Sr_2RuO_4. *Nat Commun* (2013) 4:2596. doi:10.1038/ncomms3596

60. Graf MJ, Balatsky AV. Identifying the pairing symmetry in the Sr_2RuO_4 superconductor. *Phys Rev B* (2000) 62:9697–702. doi:10.1103/PhysRevB.62.9697

61. Kotetes P, Sura HOM, Andersen BM. Anatomy of spin and current generation from magnetization gradients in topological insulators and Rashba metals. *Phys Rev B* (2023) 108:155310. doi:10.1103/PhysRevB.108.155310

62. Agterberg DF, Barzykin V, Gor'kov LP. Conventional mechanisms for exotic superconductivity. *Phys Rev B* (1999) 60:14868–71. doi:10.1103/PhysRevB.60.14868

63. Bhattacharyya A, Lees MR, Panda K, Ferreira PP, Dorini TT, Gaudry E, et al. Nodeless time-reversal symmetry breaking in the centrosymmetric superconductor $Sc_5Co_4Si_{10}$ probed by muon-spin spectroscopy. *Phys Rev Mater* (2022) 6:064802. doi:10.1103/PhysRevMaterials.6.064802

64. Stanev V, Tešanović Z. Three-band superconductivity and the order parameter that breaks time-reversal symmetry. *Phys Rev B* (2010) 81:134522. doi:10.1103/PhysRevB.81.134522

65. Carlström J, Garaud J, Babaev E. Length scales, collective modes, and type-1.5 regimes in three-band superconductors. *Phys Rev B* (2011) 84:134518. doi:10.1103/PhysRevB.84.134518

66. Maiti S, Chubukov AV. $s + is$ state with broken time-reversal symmetry in Fe-based superconductors. *Phys Rev B* (2013) 87:144511. doi:10.1103/PhysRevB.87.144511

67. Clepkens J, Lindquist AW, Kee HY. Shadowed triplet pairings in Hund's metals with spin-orbit coupling. *Phys Rev Res* (2021) 3:013001. doi:10.1103/PhysRevResearch.3.013001

68. Khodas M, Chubukov AV. Interpocket pairing and gap symmetry in Fe-based superconductors with only electron pockets. *Phys Rev Lett* (2012) 108:247003. doi:10.1103/PhysRevLett.108.247003

69. Shishidou T, Suh HG, Brydon PMR, Weinert M, Agterberg DF. Topological band and superconductivity in UTe_2. *Phys Rev B* (2021) 103:104504. doi:10.1103/PhysRevB.103.104504

70. Volovik G, Gor'kov L. Superconducting classes in heavy-fermion systems. *Eksp Teor Fiz* (1985) 88:1412.

71. Annett JF. Symmetry of the order parameter for high-temperature superconductivity. *Adv Phys* (1990) 39:83–126. doi:10.1080/00018739000101481

72. Sigrist M, Ueda K. Phenomenological theory of unconventional superconductivity. *Rev Mod Phys* (1991) 63:239–311. doi:10.1103/RevModPhys.63.239

73. Graser S, Maier TA, Hirschfeld PJ, Scalapino DJ. Near-degeneracy of several pairing channels in multiorbital models for the Fe pnictides. *New J Phys* (2009) 11: 025016. doi:10.1088/1367-2630/11/2/025016

74. Rømer AT, Kreisel A, Eremin I, Malakhov MA, Maier TA, Hirschfeld PJ, et al. Pairing symmetry of the one-band Hubbard model in the paramagnetic weak-coupling limit: a numerical RPA study. *Phys Rev B* (2015) 92:104505. doi:10.1103/PhysRevB.92.104505

75. Rømer AT, Maier TA, Kreisel A, Eremin I, Hirschfeld PJ, Andersen BM. Pairing in the two-dimensional Hubbard model from weak to strong coupling. *Phys Rev Res* (2020) 2:013108. doi:10.1103/PhysRevResearch.2.013108

76. Kreisel A, Hirschfeld PJ, Andersen BM. On the remarkable superconductivity of FeSe and its close cousins. *Symmetry* (2020) 12:1402. doi:10.3390/sym12091402

77. Røising HS, Geier M, Kreisel A, Andersen BM. Thermodynamic transitions and topology of spin-triplet superconductivity: application to UTe_2. *Phys Rev B* (2024) 109: 054521. doi:10.1103/PhysRevB.109.054521

78. Mandal M, Kataria A, Patra C, Singh D, Biswas PK, Hillier AD, et al. Time-reversal symmetry breaking in frustrated superconductor Re_2Hf. *Phys Rev B* (2022) 105:094513. doi:10.1103/PhysRevB.105.094513

79. Matsumoto M, Sigrist M. Quasiparticle states near the surface and the domain wall in a $p_x \pm ip_y$-wave superconductor. *J Phys Soc Jpn* (1999) 68:994–1007. doi:10.1143/JPSJ. 68.994

80. Stone M, Roy R. Edge modes, edge currents, and gauge invariance in p_x+ip_y superfluids and superconductors. *Phys Rev B* (2004) 69:184511. doi:10.1103/PhysRevB. 69.184511

81. Watashige T, Tsutsumi Y, Hanaguri T, Kohsaka Y, Kasahara S, Furusaki A, et al. Evidence for time-reversal symmetry breaking of the superconducting state near twin-boundary interfaces in FeSe revealed by scanning tunneling spectroscopy. *Phys Rev X* (2015) 5:031022. doi:10.1103/PhysRevX.5.031022

82. Håkansson M, Löfwander T, Fogelström M. Spontaneously broken time-reversal symmetry in high-temperature superconductors. *Nat Phys* (2015) 11:755–60. doi:10. 1038/nphys3383

83. Silaev M, Garaud J, Babaev E. Phase diagram of dirty two-band superconductors and observability of impurity-induced $s + is$ state. *Phys Rev B* (2017) 95:024517. doi:10. 1103/PhysRevB.95.024517

84. Holmvall P, Vorontsov AB, Fogelström M, Löfwander T. Broken translational symmetry at edges of high-temperature superconductors. *Nat Commun* (2018) 9:2190. doi:10.1038/s41467-018-04531-y

85. Song SY, Martiny JHJ, Kreisel A, Andersen BM, Seo J. Visualization of local magnetic moments emerging from impurities in hund's metal states of FeSe. *Phys Rev Lett* (2020) 124:117001. doi:10.1103/PhysRevLett.124.117001

86. Wennerdal NW, Ask A, Holmvall P, Löfwander T, Fogelström M. Breaking time-reversal and translational symmetry at edges of d-wave superconductors: microscopic theory and comparison with quasiclassical theory. *Phys Rev Res* (2020) 2:043198. doi:10. 1103/PhysRevResearch.2.043198

87. Stanev V, Koshelev AE. Complex state induced by impurities in multiband superconductors. *Phys Rev B* (2014) 89:100505. doi:10.1103/PhysRevB.89.100505

88. Alloul H, Bobroff J, Gabay M, Hirschfeld PJ. Defects in correlated metals and superconductors. *Rev Mod Phys* (2009) 81:45–108. doi:10.1103/RevModPhys.81.45

89. Schmid M, Andersen BM, Kampf AP, Hirschfeld PJ. d-Wave superconductivity as a catalyst for antiferromagnetism in underdoped cuprates. *New J Phys* (2010) 12:053043. doi:10.1088/1367-2630/12/5/053043

90. Gastiasoro MN, Hirschfeld PJ, Andersen BM. Impurity states and cooperative magnetic order in Fe-based superconductors. *Phys Rev B* (2013) 88:220509. doi:10.1103/PhysRevB.88.220509

91. Martiny JHJ, Gastiasoro MN, Vekhter I, Andersen BM. Impurity-induced antiferromagnetic order in Pauli-limited nodal superconductors: application to heavy-fermion $CeCoIn_5$. *Phys Rev B* (2015) 92:224510. doi:10.1103/PhysRevB.92. 224510

92. Martiny JHJ, Kreisel A, Andersen BM. Theoretical study of impurity-induced magnetism in FeSe. *Phys Rev B* (2019) 99:014509. doi:10.1103/PhysRevB.99.014509

93. Chen W, Andersen BM, Hirschfeld PJ. Theory of resistivity upturns in metallic cuprates. *Phys Rev B* (2009) 80:134518. doi:10.1103/PhysRevB.80.134518

94. Castro Neto AH, Castilla G, Jones BA. Non-fermi liquid behavior and griffiths phase in f -electron compounds. *Phys Rev Lett* (1998) 81:3531–4. doi:10.1103/PhysRevLett.81.3531

95. Millis AJ, Morr DK, Schmalian J. Local defect in metallic quantum critical systems. *Phys Rev Lett* (2001) 87:167202. doi:10.1103/PhysRevLett.87.167202

96. Das J, Mahajan AV, Bobroff J, Alloul H, Alet F, Sørensen ES. Comparison of $S = 0$ and $S=1/2$ impurities in the Haldane chain compound Y_2BaNiO_5. *Phys Rev B* (2004) 69:144404. doi:10.1103/PhysRevB.69.144404

97. Chang J, Niedermayer C, Gilardi R, Christensen NB, Rønnow HM, McMorrow DF, et al. Tuning competing orders in $La_{2-x}Sr_xCuO_4$ cuprate superconductors by the application of an external magnetic field. *Phys Rev B* (2008) 78:104525. doi:10.1103/PhysRevB.78.104525

98. Kimura H, Kofu M, Matsumoto Y, Hirota K. Novel in-gap spin state in Zn-doped $La_{1.85}Sr_{0.15}CuO_4$. *Phys Rev Lett* (2003) 91:067002. doi:10.1103/PhysRevLett.91.067002

99. Rosenthal EP. *Visualizing nematicity in the pnictides with scanning tunneling spectroscopy*. Columbia University (2015). Ph.D. thesis. doi:10.7916/D8N29W34

100. Shender EF, Kivelson SA. Dilution-induced order in quasi-one-dimensional quantum antiferromagnets. *Phys Rev Lett* (1991) 66:2384–7. doi:10.1103/PhysRevLett. 66.2384

101. Andersen BM, Hirschfeld PJ. Breakdown of universal transport in correlated d-wave superconductors. *Phys Rev Lett* (2008) 100:257003. doi:10.1103/PhysRevLett. 100.257003

102. Christensen RB, Hirschfeld PJ, Andersen BM. Two routes to magnetic order by disorder in underdoped cuprates. *Phys Rev B* (2011) 84:184511. doi:10.1103/PhysRevB.84. 184511

103. Schmid M, Loder F, Kampf AP, Kopp T. Disorder induced stripes in d-wave superconductors. *New J Phys* (2013) 15:073049. doi:10.1088/1367-2630/15/7/073049

104. Kivelson SA, Bindloss IP, Fradkin E, Oganesyan V, Tranquada JM, Kapitulnik A, et al. How to detect fluctuating stripes in the high-temperature superconductors. *Rev Mod Phys* (2003) 75:1201–41. doi:10.1103/RevModPhys.75.1201

105. Vojta M. Lattice symmetry breaking in cuprate superconductors: stripes, nematics, and superconductivity. *Adv Phys* (2009) 58:699–820. doi:10.1080/00018730903122242

106. Lake B, Rønnow HM, Christensen NB, Aeppli G, Lefmann K, McMorrow DF, et al. Antiferromagnetic order induced by an applied magnetic field in a high-temperature superconductor. *Nature* (2002) 415:299–302. doi:10.1038/415299a

107. Khaykovich B, Lee YS, Erwin RW, Lee SH, Wakimoto S, Thomas KJ, et al. Enhancement of long-range magnetic order by magnetic field in superconducting La_2CuO_{4+y}. *Phys Rev B* (2002) 66:014528. doi:10.1103/PhysRevB.66.014528

108. Rømer AT, Chang J, Christensen NB, Andersen BM, Lefmann K, Mähler L, et al. Glassy low-energy spin fluctuations and anisotropy gap in $La_{1.88}Sr_{0.12}CuO_4$. *Phys Rev B* (2013) 87:144513. doi:10.1103/PhysRevB.87.144513

109. Watanabe I, Adachi T, Takahashi K, Yairi S, Koike Y, Nagamine K. Muon-spin-relaxation study of the effect of nonmagnetic impurities on the Cu-spin fluctuations in $La_{2-x}Sr_xCu_{1-y}Zn_yO_4$ around $x = 0.115$. *Phys Rev B* (2002) 65:180516. doi:10.1103/PhysRevB.65.180516

110. Khaykovich B, Wakimoto S, Birgeneau RJ, Kastner MA, Lee YS, Smeibidl P, et al. Field-induced transition between magnetically disordered and ordered phases in underdoped $La_{2-x}Sr_xCuO_4$. *Phys Rev B* (2005) 71:220508. doi:10.1103/PhysRevB.71. 220508

111. Niedermayer C, Bernhard C, Blasius T, Golnik A, Moodenbaugh A, Budnick JI. Common phase diagram for antiferromagnetism in $la_{2-x}Sr_xCuO_4$ and $Y_{1-x}Ca_xBa_2Cu_3O_6$ as seen by muon spin rotation. *Phys Rev Lett* (1998) 80:3843–6. doi:10.1103/PhysRevLett.80.3843

112. Panagopoulos C, Tallon JL, Rainford BD, Xiang T, Cooper JR, Scott CA. Evidence for a generic quantum transition in high-T_c cuprates. *Phys Rev B* (2002) 66:064501. doi:10.1103/PhysRevB.66.064501

113. Miller RI, Kiefl RF, Brewer JH, Callaghan FD, Sonier JE, Liang R, et al. Coexistence of magnetism and superconductivity in ultraclean underdoped $YBa_2Cu_3O_{6.37}$. *Phys Rev B* (2006) 73:144509. doi:10.1103/PhysRevB.73.144509

114. Haug D, Hinkov V, Suchaneck A, Inosov DS, Christensen NB, Niedermayer C, et al. Magnetic-field-enhanced incommensurate magnetic order in the underdoped high-temperature superconductor $YBa_2Cu_3O_{6.45}$. *Phys Rev Lett* (2009) 103:017001. doi:10.1103/PhysRevLett.103.017001

115. Pan SH, Hudson EW, Lang KM, Eisaki H, Uchida S, Davis JC. Imaging the effects of individual zinc impurity atoms on superconductivity in $Bi_2Sr_2CaCu_2O_{8+\delta}$. *Nature* (2000) 403:746–50. doi:10.1038/35001534

116. Sundar S, Azari N, Goeks MR, Gheidi S, Abedi M, Yakovlev M, et al. Ubiquitous spin freezing in the superconducting state of UTe_2. *Comm Phys* (2023) 6:24. doi:10. 1038/s42005-023-01146-8

117. Azari N, Yakovlev M, Rye N, Dunsiger SR, Sundar S, Bordelon MM, et al. Absence of spontaneous magnetic fields due to time-reversal symmetry breaking in bulk superconducting UTe_2. *Phys Rev Lett* (2023) 131:226504. doi:10.1103/PhysRevLett.131.226504

118. Inosov DS, Friemel G, Park JT, Walters AC, Texier Y, Laplace Y, et al. Possible realization of an antiferromagnetic Griffiths phase in $Ba(Fe_{1-x}Mn_x)_2As_2$. *Phys Rev B* (2013) 87:224425. doi:10.1103/PhysRevB.87.224425

119. Gastiasoro MN, Andersen BM. Enhancement of magnetic stripe order in iron-pnictide superconductors from the interaction between conduction electrons and magnetic impurities. *Phys Rev Lett* (2014) 113:067002. doi:10.1103/PhysRevLett.113. 067002

120. Urbano RR, Young BL, Curro NJ, Thompson JD, Pham LD, Fisk Z. Interacting antiferromagnetic droplets in quantum critical $CeCoIn_5$. *Phys Rev Lett* (2007) 99: 146402. doi:10.1103/PhysRevLett.99.146402

121. Li Y, Sapkota A, Lozano PM, Du Z, Li H, Wu Z, et al. Strongly overdoped $La_{2-x}Sr_xCuO_4$: evidence for Josephson-coupled grains of strongly correlated superconductor. *Phys Rev B* (2022) 106:224515. doi:10.1103/PhysRevB.106.224515

122. Maier TA, Karakuzu S, Scalapino DJ. Overdoped end of the cuprate phase diagram. *Phys Rev Res* (2020) 2:033132. doi:10.1103/PhysRevResearch.2.033132

123. Balatsky AV, Vekhter I, Zhu JX. Impurity-induced states in conventional and unconventional superconductors. *Rev Mod Phys* (2006) 78:373–433. doi:10.1103/RevModPhys.78.373

124. Holbæk SC, Christensen MH, Kreisel A, Andersen BM. Unconventional superconductivity protected from disorder on the kagome lattice. *Phys Rev B* (2023) 108:144508. doi:10.1103/PhysRevB.108.144508

125. Pal M, Bettmann L, Kreisel A, Hirschfeld PJ. Magnetic anisotropy from strain-induced dislocations in correlated electron systems. *Phys. Rev. B* (2021) 103:245132. doi:10.1103/PhysRevB.103.245132

126. Pal M, Kreisel A, Hirschfeld PJ. Topological superconductivity driven by correlations and linear defects in multiband superconductors. *Phys. Rev. B* (2023) 107:134503. doi:10.1103/PhysRevB.107.134503

127. Ruderman MA, Kittel C. Indirect exchange coupling of nuclear magnetic moments by conduction electrons. *Phys Rev* (1954) 96:99–102. doi:10.1103/PhysRev. 96.99

128. Kasuya T. A theory of metallic ferro- and antiferromagnetism on zener's model. *Prog Theor Phys* (1956) 16:45–57. doi:10.1143/PTP.16.45

129. Yosida K. Magnetic properties of Cu-Mn alloys. *Phys Rev* (1957) 106:893–8. doi:10.1103/PhysRev.106.893

130. Abrikosov A. (1988).*Fundamentals of the theory of metals*. Fundamentals of the Theory of Metals (North-Holland

131. Aristov DN, Maleyev SV, Yashenkin AG. RKKY interaction in layered superconductors with anisotropic pairing. *Z für Physik B Condensed Matter* (1997) 102:467–71. doi:10.1007/s002570050313

132. Galitski VM, Larkin AI. Spin glass versus superconductivity. *Phys Rev B* (2002) 66:064526. doi:10.1103/PhysRevB.66.064526

133. Schecter M, Flensberg K, Christensen MH, Andersen BM, Paaske J. Self-organized topological superconductivity in a Yu-Shiba-Rusinov chain. *Phys Rev B* (2016) 93:140503. doi:10.1103/PhysRevB.93.140503

134. Yu L. Bound state in superconductors with paramagnetic impurities. *Acta Physica Sinica* (1965) 21:75–91. doi:10.7498/aps.21.75

135. Shiba H. Classical spins in superconductors. *Prog Theor Phys* (1968) 40:435–51. doi:10.1143/PTP.40.435

136. Rusinov A. Theory of gapless superconductivity in alloys containing paramagnetic impurities. *Sov Phys JETP* (1969) 29:1101–6.

137. Yao NY, Glazman LI, Demler EA, Lukin MD, Sau JD. Enhanced antiferromagnetic exchange between magnetic impurities in a superconducting host. *Phys Rev Lett* (2014) 113:087202. doi:10.1103/PhysRevLett.113.087202

138. Hoffman S, Klinovaja J, Meng T, Loss D. Impurity-induced quantum phase transitions and magnetic order in conventional superconductors: competition between bound and quasiparticle states. *Phys Rev B* (2015) 92:125422. doi:10.1103/PhysRevB.92.125422

139. Fittipaldi R, Hartmann R, Mercaldo MT, Komori S, Bjørlig A, Kyung W, et al. Unveiling unconventional magnetism at the surface of Sr_2RuO_4. *Nat Commun* (2021) 12:5792. doi:10.1038/s41467-021-26020-5

140. Blundell S, De Renzi R, Lancaster T, Pratt F. *Muon spectroscopy: an introduction*. Oxford University Press (2022).

141. Sonier JE, Brewer JH, Kiefl RF. μSR studies of the vortex state in type-II superconductors. *Rev Mod Phys* (2000) 72:769–811. doi:10.1103/RevModPhys.72.769

142. Khasanov R, Guguchia Z. Probing the multi gap behavior within '11' and '122' families of iron based superconductors: the muon-spin rotation studies. *Superconductor Sci Technol* (2015) 28:034003. doi:10.1088/0953-2048/28/3/034003

143. Curran PJ, Bending SJ, Gibbs AS, Mackenzie AP. The search for spontaneous edge currents in Sr_2RuO_4 mesa structures with controlled geometrical shapes. *Scientific Rep* (2023) 13:12652. doi:10.1038/s41598-023-39590-9

144. Mueller E, Iguchi Y, Watson C, Hicks CW, Maeno Y, Moler KA. Constraints on a split superconducting transition under uniaxial strain in Sr_2RuO_4 from scanning SQUID microscopy. *Phys Rev B* (2023) 108:144501. doi:10.1103/PhysRevB.108.144501

145. Huddart BM, Onuorah IJ, Isah MM, Bonfà P, Blundell SJ, Clark SJ, et al. Intrinsic nature of spontaneous magnetic fields in superconductors with time-reversal symmetry breaking. *Phys Rev Lett* (2021) 127:237002. doi:10.1103/PhysRevLett.127.237002

146. Blundell SJ, Lancaster T. DFT + μ: density functional theory for muon site determination. *Appl Phys Rev* (2023) 10:021316. doi:10.1063/5.0149080

147. Miyake K, Tsuruta A. Theory for intrinsic magnetic field in chiral superconductor measured by muSR: case of Sr_2RuO_4. arXiv e-prints (2017) 1709.09388. doi:10.48550/arXiv.1709.09388

148. Schemm E, Levenson-Falk E, Kapitulnik A. Polar Kerr effect studies of time reversal symmetry breaking states in heavy fermion superconductors. *Physica C: Superconductivity its Appl* (2017) 535:13–9. doi:10.1016/j.physc.2016.11.012

149. Hayes IM, Wei DS, Metz T, Zhang J, Eo YS, Ran S, et al. Multicomponent superconducting order parameter in UTe_2. *Science* (2021) 373:797–801. doi:10.1126/science.abb0272

150. Ajeesh MO, Bordelon M, Girod C, Mishra S, Ronning F, Bauer ED, et al. Fate of time-reversal symmetry breaking in UTe_2. *Phys Rev X* (2023) 13:041019. doi:10.1103/PhysRevX.13.041019

151. Xia J, Maeno Y, Beyersdorf PT, Fejer MM, Kapitulnik A. High resolution polar Kerr effect measurements of Sr_2RuO_4: evidence for broken time-reversal symmetry in the superconducting state. *Phys Rev Lett* (2006) 97:167002. doi:10.1103/PhysRevLett.97.167002

152. Cho W, Kivelson SA. Necessity of time-reversal symmetry breaking for the polar Kerr effect in linear response. *Phys Rev Lett* (2016) 116:093903. doi:10.1103/PhysRevLett.116.093903

153. Yip SK, Sauls JA. Circular dichroism and birefringence in unconventional superconductors. *J Low Temperature Phys* (1992) 86:257–90. doi:10.1007/BF01151804

154. Taylor E, Kallin C. Intrinsic Hall effect in a multiband chiral superconductor in the absence of an external magnetic field. *Phys Rev Lett* (2012) 108:157001. doi:10.1103/PhysRevLett.108.157001

155. Goryo J. Impurity-induced polar Kerr effect in a chiral *p*-wave superconductor. *Phys Rev B* (2008) 78:060501. doi:10.1103/PhysRevB.78.060501

156. Lutchyn RM, Nagornykh P, Yakovenko VM. Frequency and temperature dependence of the anomalous ac Hall conductivity in a chiral $p_x + ip_y$ superconductor with impurities. *Phys Rev B* (2009) 80:104508. doi:10.1103/PhysRevB.80.104508

157. Liu HT, Chen W, Huang W. Impact of random impurities on the anomalous Hall effect in chiral superconductors. *Phys Rev B* (2023) 107:224517. doi:10.1103/PhysRevB.107.224517

158. Palle G, Hicks C, Valenti R, Hu Z, Li YS, Rost A, et al. Constraints on the superconducting state of Sr_2RuO_4 from elastocaloric measurements. *Phys Rev B* (2023) 108:094516. doi:10.1103/PhysRevB.108.094516

159. Theuss F, Shragai A, Grissonnanche G, Hayes IM, Saha SR, Eo YS, et al. Single-component superconductivity in UTe_2 at ambient pressure. *arXiv e-prints* (2023):10938. doi:10.48550/arXiv.2307.10938